Heterologous Expression of Mycobacterium tuberculosis Virulence Factor, Mtb-BrkB, in *Escherichia coli*

Stefanie Dejneka
Biochemistry and Molecular Biology Program
Lake Forest College
Lake Forest, Illinois 60045

Tuberculosis (TB) infection is caused by bacterial pathogen *Mycobacterium tuberculosis* (Mtb). While treatments for TB exist, it remains the world's deadliest infectious disease, killing more than 1 million people a year. Although antibiotic treatments for tuberculosis exist, their longevity and inaccessibility, as well as the rise of drug-resistant tuberculosis (DRTB) means that antibiotic treatment alone are not widely effective. Therefore, new avenues of combatting TB are required by targeting specific, understudied virulence factors in Mtb. Mtb-BrkB is a 35kDa protein in *Mycobacterium tuberculosis* which has been shown to promote virulence. When Mmar-BrkB, the *Mycobacterium marinum* ortholog of Mtb-BrkB, is mutated in *Mycobacterium marinum*, infection in zebrafish is attenuated. The goal of this project is to express and isolate Mtb-BrkB for the purpose of downstream structural and functional analysis. The Mtb-BrkB-6XHis protein was recombinantly expressed in *E. coli.* The cells were subsequently lysed and Ni-NTA resin affinity chromatography was used to isolate the protein. Analysis of presence and purity of protein was determined by SDS-PAGE and Western Blot using mouse monoclonal anti-6XHis antibodies. The future directions of this research include a scaled-up production of Mtb-BrkB, a multimerization assay to determine the quaternary structure of Mtb-BrkB, and structural analysis by cryo-electron microscopy.

Introduction

Bacteria are plentiful in the soil, water, air, and even the human body. Many of these bacteria do humans no harm and can even help with bodily processes such as digestion. However, some bacteria have specially evolved to invade, live, and multiply within human hosts. These bacteria are pathogenic, or disease causing. While human pathogens, including viruses, fungi, bacteria, and others, are relatively small in number, with only 1513 reported species of bacteria which can infect humans (Bartlett et al., 2022) out of a predicted total of between 10^{11}-10^{12} microbial species on earth (Locey & Lennon, 2016), their effect on global health can be immense. In 2019, 7.7 million deaths were associated with bacterial infection (GBD 2019 Antimicrobial Resistance Collaborators, 2022). Bacteria which are pathogenic rely on virulence factors, cellular machinery, molecules, and regulatory factors which allow pathogens to invade, survive, and evade immune response in a host.

One such pathogenic bacteria is *Mycobacterium tuberculosis*, discovered in 1882 by Robert Koch to be the bacterium responsible for tuberculosis infection (Koch et al., 1882). *M. tuberculosis* is an obligate pathogen, meaning it cannot survive outside of a host. Within a host, *M. tuberculosis* takes advantage of the hosts immune response to survive and multiply. While the bacterial cause of tuberculosis was only discovered in 1882, it is an ancient disease that has long plagued humanity, with the earliest written record of tuberculosis infection dating back 3300 years (Barberis et al., 2017). Despite an available vaccine and antibiotic treatment, tuberculosis continues to infect people around the world, causing more deaths than any other infectious disease. By studying how tuberculosis so effectively infects humans, we can continue to strive towards new strategies to combat and eradicate tuberculosis. In order to target *mycobacterium tuberculosis*, it is important to understand the etiology, the global burden of disease, the characteristics of the disease-causing bacterium, and mechanisms of disease transmission in order to move forward with new solutions.

Tuberculosis: The Disease

Tuberculosis (TB) is an infectious disease caused by *Mycobacterium tuberculosis* (Koch, 1882). The most prevalent type of TB is pulmonary TB, which infects the lungs and is spread primarily by an infected individual coughing the bacterium through the air. In 2024, 80% of all TB cases were pulmonary TB, compared to just 19% of cases were extrapulmonary (VidyaRaj, C.K., 2025). Extrapulmonary TB infects cells outside of the lungs such as in the blood stream, causing miliary TB, the kidneys, causing genitourinary TB, the lymph nodes causing tuberculosis lymphadenitis, etc. Pulmonary TB symptoms include a cough which lasts 3 weeks or longer, chest pain, coughing blood or phlegm, fever, fatigue, and weight loss, which all worsen with time. Risk factors of TB include HIV/AIDS, diabetes, malnutrition, chemotherapy, severe kidney disease, misuse of alcohol, and use of steroids or tobacco products (Mayo Clinic 2023).

While TB is treatable by antibiotics, inaccessibility and drug-resistance contribute the continued prevalence of the disease. Current TB treatment includes a drug regimen of 4-9 months (CDC 2020). The first line drugs used for drug-responsive TB include Isoniazid, Rifampicin, Pyrazinamide, and Ethambutol. The second-line TB drugs for drug resistant TB include Bedaquiline, Cycloserine, and Kanamycin. While drugs show cure rates as high as 95% in clinical trials, in actual treatment programs their performance is much worse due to high patient dropout rates (Bendre et. al. 2021). Current TB drug regimens have a very long course of treatment, which is often inaccessible to patients leading to the early termination of drug regimens. Incomplete courses of antibiotics can increase the risk of drug-resistance and relapse.

The prevalence of drug-resistant TB is a growing issue. Drug resistance is caused by the acquisition of mutations which allow for antibiotic resistance. This can be caused by incomplete or inadequate antibiotic treatment, and then spread by normal mechanisms of transmission. There are two classes of drug resistant TB: multi-drug resistant TB (MDR-TB) which is resistant to first line drugs such as isoniazid and rifampicin and extensively drug resistant TB (XDR-TB) which are resistant to first and some second line drugs (Gandhi et al., 2010). The global rate of MDR-TB is 11.6% of all TB cases (Salari et al., 2023). Drug resistant TB is a major global health problem because it is more difficult to treat that drug responsive TB, and existing TB solutions and antibiotics are ineffective against it. The course of antibiotics to treat MDR-TB can take between 18-24 months (Gandhi et al., 2010). Therefore, new solutions including increased accessibility of treatment and new chemotherapies for tuberculosis are necessary in the face of rising drug-resistance.

The Bacille Calmette-Guérin vaccine (BCG) is a prophylaxis for TB. It was developed in 1921 from Mycobacterium bovis, a bovine strain of tuberculosis, by Albert Calmette and Camille Guérin. The French scientists cultured a virulent strain of M. bovis on potatoes until virulence was lost or attenuated (Luca & Mihaescu, 2013). The BCG vaccine is still administered in countries with high rates of TB; however, its efficacy is variable. While it is effective at preventing extrapulmonary TB in children under 5, it is less effective at protecting against pulmonary TB in adults (Bendre et al., 2021). Because most TB cases are pulmonary TB, this vaccine is not adequate as the sole protection against TB.

The Global Health Burden of TB

Globally, 10.8 million people got tuberculosis in 2023, and 1.25 million died from the disease (WHO 2024). Despite available treatment options, TB continues to be the deadliest infectious disease worldwide, with the exception of the years 2020-2022 when COVID-19 surpassed TB in the number of deaths. Additionally, the global burden of TB is not being shouldered equally. TB is not geographically neutral; most of the TB incidences are in South-East Asia, Africa, and the Western Pacific. The 30 highest TB burdened countries shoulder 87% of the worldwide TB burden in 2023, with just 8 of these countries, India, Indonesia, China, the Philippines, Pakistan, Nigeria, Bangladesh, and the Democratic Republic of Congo, accounting for over 60% of the worldwide TB incidence (WHO

*This author wrote this paper as a senior thesis under the direction of Dr. William H. Conrad

2024). In 2023, the United States reported only 9,633 cases of TB, which is 0.08% of the global total, however, incidence rose 15.6% from 2022 (CDC, 2024). Therefore, while TB incidence is low in the US, it is still prevalent and the deadliest infectious disease in the world. Moreover, the disease burden of TB is shouldered disproportionately by the Global South and countries that may struggle to afford the high cost of lengthy TB treatment.

High burden countries face higher rates of TB incidence due to the high rates of poverty which lead to undernutrition, increased transmission due to overcrowding, and inability to pay the cost of treatment for TB. There is an inverse correlation between a country's GDP and TB incidence per 100,000 people. One of the highest risk factors for TB is undernutrition, which accounted for about 1 million new cases of TB in 2023 (WHO 2024). As well, overcrowding, poor ventilation, and in house TB contact are risk factors for TB and lead to disease transmission (Lee, J. et. al., 2022). This suggest that poverty is a risk factor for tuberculosis, and TB disproportionately affects those who are impoverished and undernourished.

Low-income countries, which are more likely to have new cases of TB, also are less likely to be able to shoulder the cost of treatment. In India, which accounts for 26% of TB cases (WHO 2024), the burden of cost shouldered by patients can be extremely high. Between 2000 and 2018 in India, catastrophic costs, defined as costs over 20% of total annual household income, affected between 7% and 32.4% of patients with drug-responsive TB and 68% of patients with drug-resistant TB (Chandra et al., 2020). These costs only plunge families struggling with tuberculosis further into poverty. Current TB treatment is often long, inaccessible and complex for low-income countries which are most effected by TB.

Moreover, low-income countries face greater difficulties in providing timely treatment for TB. The delayed diagnosis of TB can lead to delayed treatment and further transmission of the disease. In low-income and low-middle-income countries the median patient delays due to financial, physical and social difficulties of seeking treatment was 28 days. The median healthcare delay, which is caused by complicated administrative processes, referral systems, and delay in diagnosis, in low-income and low-middle-income countries was 14 days. The median treatment delay in low-income and low-middle income countries was found to be 14 days. This brings the total delay to about 56 days compared to a total delay of about 14 days in upper-middle income countries (Teo et al., 2021). This lengthy delay from onset of symptoms until the beginning of treatment shows disparities of treatment in low-income countries and may allow for the continued transmission of TB prior to treatment. More work needs to be done in order to make TB treatment accessible and reduce delays.

Tuberculosis: The Bacterium

Mycobacterium tuberculosis (M.tb) is a pathogenic bacterium discovered in 1882 by Robert Koch. It is a bacillus or rod-shaped bacterium of the *Mycobactericeae* family. It has a very unique cell wall structure containing mycolic acids, which give the *Mycobactericeae* family its name. Typically, bacteria fall into either the gram-positive or gram-negative cell wall category. The basic structure of the cell wall of a gram-negative bacterium includes an inner cell membrane, an outer membrane, and peptidoglycan or other lipoproteins or glycoproteins within the periplasmic space between the membranes. The basic structure of a gram-positive bacterium includes an inner membrane and a thick layer of peptidoglycan surrounding the cell. The mycobacterial cell envelope is extremely complex (Figure 1). It contains an inner plasma membrane and a rigid peptidoglycan layer, between which sits the periplasmic space. The plasma membrane functions to regulate cellular intake of nutrients and it is the location of cell wall synthesis (Lee et al., 1996). The plasma membrane is made up of a typical phospholipid bilayer, but also contains phosphatidylinositol mannosides (PIMs), and lipomannans (LMs). PIMs may cause the mycobacterial membrane to be less permeable, decreasing susceptibility to antibiotics (Dulberger et al., 2020). Peptidoglycan maintains cell structure and shape. Arabinogalactan is a branched sugar molecule that forms the link between the mycomembrane and peptidoglycan. Lipoaribomannans (LAMs) are anchored in the plasma membrane and covalently attached to the arabinogalactan sugars, and they are an important part of the mycobacterial envelope's structural integrity. The mycolic acids which give mycobacteria their name form the outer membrane of the mycobacterial cell envelope, and they also help to make the mycobacterial cell wall less permeable to antibiotics. The mycomembrane is 100-1000 times less permeable to b-lactam antibiotics than a gram negative envelope (Dulberger et al., 2020). Therefore, the thickness and complexity of the mycobacterial cell envelope plays a role in *M. tuberculosis* survival and impermeability to antibiotics. The mycomembrane is composed of the inner leaflet of mycolic acids covalently attached to the arabinogalactan sugars, and an outer leaflet which is attached to trehalose monomycolate (TMM) and trehalose dimycolate (TDM) sugars which are on the surface of the mycomembrane (Dulberger et al., 2020). As well the outer mycobacterial membrane contains phthiocerol dimycocerosates (PDIMs) on the surface. PDIMs may interfere with immune recognition of pathogen associated molecular patterns (PAMPs), inhibiting detection of *Mycobacteria* and immune response (Cambier, Takaki, et al., 2014). Therefore, the mycobacterial cell membrane is not only structurally important but also helps *M. tuberculosis* survive within the host.

Mycobacterial cell growth depends on cell wall synthesis. Mtb has two different growth stages. The first is rapid growth which occurs when there is little stress and excess nutrients. The second is growth stasis in which *M. tuberculosis* replicates slowly and experiences stress. Most of the cell envelope lipid synthesis is upregulated during rapid growth and downregulated during growth stasis phases including PIMs which make up the plasma membrane and the mycolic acids and trehalose sugars which make up the mycomembrane (Dulberger et al., 2020). However, LAM and LM synthesis is upregulated during starvation (Betts et al., 2002), indicating that they are more abundant in slow growth phases, and may have a role in protecting mycobacteria in the stressful intracellular growth environment. Many antibiotics which target *mycobacterium tuberculosis* target different parts of the cell wall synthesis. Isoniazid targets mycolic acid synthesis, and ethambutol target arabinogalactan synthesis (Dulberger et al., 2020). Since the cell wall synthesis is necessary for Mtb to replicate, these antibiotics are bacteriostatic or stop bacterial growth.

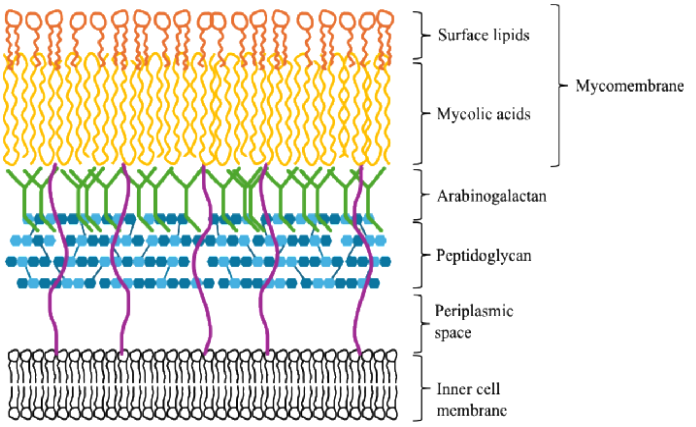

Figure 1. The mycobacterial cell envelope.
The mycobacterial cell envelope has a unique structure that contains an inner cell membrane (black), peptidoglycan (blue), lipoaribomannan (purple) arabinogalactan (green), and the mycolic acids (yellow) and surface lipids (orange) which are characteristic of the *Mycobactericeae* family.

Tuberculosis Model of Pathogenesis and Transmission

Tuberculosis continues to infect and kill millions of people globally not only because of global health initiative shortcomings, but also because tuberculosis is a skilled pathogen. It is able to survive many different intracellular and extracellular environments within the host, evade immune response, and recruit immune cells in order to create a survival niche. The path of TB transmission and infection typically follows the steps: 1) entry into a new host through the lungs, 2) infection of a macrophage, 3) formation of a granuloma and intracellular replication, 4) granuloma maturation, and

5) granuloma necrosis and extracellular replication. The cycle complete with transmission of bacterium from infected host to a new host (Figure 2).

TB is an airborne pathogen which is spread through tiny droplets containing 1-3 bacterium through coughing from the source infection to a new host. When the new host inhales the droplets, they may become infected with tuberculosis. Infection is initiated in the lower lung, which provides the host niche that tuberculosis needs to survive. The droplet size of tuberculosis infectious is inversely correlated with infection (Ratcliffe & Wells, 1948). Therefore, a larger bacterial burden in a larger droplet is less successful because it cannot reach the lower alveolar space.

Once it has entered the lungs, TB avoids detection by the host immune response by secreting a surface lipid, phthiocerol dimycoceroserate (PDIM), that masks pathogen associated molecular patterns (PAMPs) or markers which the immune system recognizes as pathogenic and activates immune response. Simultaneously, TB recruits' macrophages that are growth-permissive by secreting phenolic glycolipid (PGL) which activates macrophage chemokine *CCL2* which recruits macrophages (Cambier, Falkow, et al., 2014). This strategy at once hides from the immune response and recruits macrophages which are growth-permissive works well in the lower lung where there is relatively low microbial and immune club. Therefore, mycobacterium tuberculosis requires surface lipids in order to evade host immune response and infiltrate host macrophages.

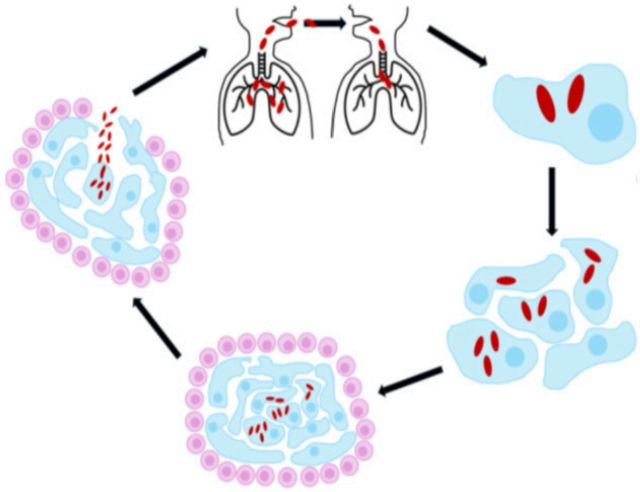

Figure 2. Mycobacterium tuberculosis path of infection and transmission.

Mycobacterium transmission is initiated by the transfer of airborne droplets from an infected individual's lungs to an uninfected individual's lungs. The bacteria are then engulfed by a macrophage, in which they can divide. More macrophages are recruited to the infection and the granuloma begins to form. A mature granuloma recruits lymphocytes which form an epithelial-like layer around a necrotic center. Finally, the granuloma bursts and releases the mycobacteria tuberculosis bacteria into the extracellular space of the infected individual's lungs.

Once it has entered the lungs, TB avoids detection by the host immune response by secreting a surface lipid, phthiocerol dimycoceroserate (PDIM), that masks pathogen associated molecular patterns (PAMPs) or markers which the immune system recognizes as pathogenic and activates immune response. Simultaneously, TB recruits' macrophages that are growth-permissive by secreting phenolic glycolipid (PGL) which activates macrophage chemokine *CCL2* which recruits macrophages (Cambier, Falkow, et al., 2014). This strategy at once hides from the immune response and recruits macrophages which are growth-permissive works well in the lower lung where there is relatively low microbial and immune club. Therefore, mycobacterium tuberculosis requires surface lipids in order to evade host immune response and infiltrate host macrophages.

Tuberculosis must then survive and replicate within the macrophages. The Mycobacterium tuberculosis is phagocytosed by the macrophage. The phagosome is a vesicle that digests pathogens and foreign particles. Therefore, TB must be able to survive or avoid acidification by the phagosome. TB escapes the phagosome into the cytosol of the macrophage and replicates within this intracellular environment.

Mycobacterium tuberculosis then recruits other macrophages to form a granuloma, an ability that is predicated on the ESX-1 efflux pump. A granuloma is a cluster of immune cells that forms an epithelial-like layer around the infected core. This protective layer was thought to contain tuberculosis to stop its spread, but it also acts as a protected environmental niche in which tuberculosis can multiply. Granulomas form when the infected macrophages undergo apoptosis, or cell death, and recruit more macrophages to engulf the dying cell and bacteria. This process repeats to form a mass of macrophage cells that expands the niche of the Mtb, allowing it to divide rapidly in early infection. The internal environment of macrophages is toxic to Mtb. One reason Mtb is able to survive in the intracellular environment of the macrophages is the virulence factor, ESX-1. As well, Mtb has the unique ability to synthesize tryptophan.

Once, a granuloma has formed it shifts from apoptotic cell death of the macrophages into necrosis of the macrophages. Apoptosis keeps to cell membrane of the macrophages intact, keeping Mtb encased within the cell, while necrosis leads to the lysis or breaking up of the cell. This creates a granuloma with a necrotic core, which provides a good extracellular environment for Mtb to replicate. The mechanism of macrophage necrosis may be triggered by host dysregulation of TNF, or tumor necrosis factor. Because of the necrosis of the granuloma, and Mtb's rapid replication, Mtb is able to escape the granuloma into the lungs. There the bacteria are aerosolized into droplets and are able to be transmitted into a new host through coughing or sneezing.

Targeting TB Requires New Solutions

While the mechanism of TB infection are well-studied and antibiotic treatments exist, TB remains a global health issue because current therapies, prevention, and public health strategies have not overcome the burden of poverty. TB prevalence is highly associated with poverty and social determinants of health. Therefore, new solutions to address TB globally must address alleviating poverty and providing direct assistance to countries and individuals with high TB burdens. Providing a basic income to patients affected by TB can improve health outcomes and reduce the risk of incurring catastrophic treatment costs. In Peru, TB-affected household which received intervention in the form of monthly cash transfers (an average of US$137 per household over the total course of treatment) in addition to traditional TB treatment were less likely to have catastrophic costs over the course of TB treatment than those without intervention (Wingfield et al., 2016). Therefore, providing even small monthly payments of financial aid to TB-affected household can help alleviate costs of treatment and prevent catastrophic financial hardship. As well, this economic intervention improved health outcomes. In the intervention group, treatment was successful for 64% of patients compared to 53% of patients in the non-intervention or control group (Wingfield et al., 2017). This suggests that alleviating poverty and the barrier of cost of treatment improves health outcomes in patients with TB.

Malnutrition is one of the prominent risk factors associated with TB

Malnutrition is also associated with poverty and access to food. In Brazil, patients who were given health care coupled with monthly food vouchers to had 13% greater rate of being cured compared to patients who only received traditional TB treatment (Reis-Santos et al., 2022). This suggests that providing adequate nutrition to TB patients who might not otherwise have access to it improves health outcomes. Therefore, socioeconomic interventions have a positive effect on the effectiveness of TB treatment.

Directly Observed Therapy Short course (DOTS) is a strategy for TB treatment developed by the World Health Organization that involves political commitment, timely diagnosis through sputum microscopy,

a six-to-eight-month standardized treatment regimen with directly observed treatment for at least two months, a regular supply of anti-TB drugs, and a standardized recording and reporting system to track patient progress. DOTS has been shown to improve cure rates of TB and decrease failure rates due to drug resistance in China ("Results of Directly Observed Short-Course Chemotherapy in 112,842 Chinese Patients with Smear-Positive Tuberculosis. China Tuberculosis Control Collaboration," 1996). The DOTS strategy has received some controversy for the direct observation of treatment parameter, which requires a healthcare worker to directly observe that anti-TB drugs have been taken by the patient. This method is considered paternalistic and may not be effective. In Pakistan, patients who received treatment according to WHO guidelines with either healthcare worker observation family member observation, or no observation did not show significant difference in cure rates (Walley et al., 2001). Therefore, the success of the DOTS strategy is most likely due to the earlier diagnosis and strengthened and standardized level of care rather than the direct observation of treatment.

While addressing social determinants of health can greatly improve treatment outcomes, another route to eradicating TB is prophylaxis or preventative treatment and vaccines. The Bacille Calmette-Guerin vaccine is currently the only vaccine for tuberculosis, and as previously discussed, it is largely ineffective at treating pulmonary TB in adults. While about 16 other vaccine options are under different phases of clinical trials, none have been officially licensed. The rBCG or AERAS-422 vaccine trails were terminated despite showing increased anti-mycobacterial activity because of association with varicella zoster virus, which can cause shingles in adults, in two cases after administration (Hoft et al., 2016). Another vaccine candidate, which entered phase two trials, the MVA85A which expresses the *M. tuberculosis* antigen 85A was found to be safe and well tolerated by patients but did not increase efficacy of protection compared to the BCG vaccine (Ndiaye et al., 2015). A promising vaccine candidate is the MIP vaccine which was originally developed in India for leprosy, but has shown to increase immune response taken in conjunction with the BCG vaccine in comparison to only BCG in mice (Saqib et al., 2016). However, these effects have not yet been studied in human trials. Therefore, new vaccine options must continue to be explored if an effective prophylaxis for pulmonary tuberculosis is to be found.

As well, in order to address the rising problem of drug-resistant TB, new chemotherapeutic solutions are needed. In order to develop new antibiotics, new drug target candidates must be identified and examined. These drug targets are virulence factors, or molecules that enable pathogens to invade the host, evade the immune system, and replicate within the host. Some new drug targets have been identified including GyrA, a DNA gyrase which catalyzes DNA supercoiling, DnaN, a subnit of DNA polymerase III, Pks13, which is essential for mycolic acid synthesis, and others (Huszár et al., 2020). These novel drug targets are promising avenues to new drug candidates; however, the process of drug discovery is complex and it is important to continue to search for novel drug targets. Because *M. tuberculosis* has a complex mechanism of pathogenesis and survives in multiple environmental niches, an ideal drug candidate would target a virulence factor that contributes to both intracellular and extracellular survival of Mtb in the host.

Mtb-BrkB: A Possible Virulence Factor

Mtb-BrkB is an Mtb putative transporter protein also known as Rv2707, according to the H37Rv Mtb reference genome. Its function is currently unknown; however, it is a protein of interest because it was found to promote Mtb growth in mice in a transposon screen. The Rv2707 transposon mutant Mtb growth was attenuated over 4-fold in mice (Sassetti & Rubin, 2003) (Fig. 3). Because a disruption in Rv2707 or Mtb-BrkB causes attenuated infection in mice, Mtb-BrkB is likely to play a role in the in vivo survival of Mtb and its virulence. Mtb-BrkB is so called because it contains the *Bordetella* resistance to complement-mediated killing (BrkB) domain. The *Bordetella pertussis* BrkB (Bp-BrkB) is a virulence factor which was found to be necessary for serum resistance in *B. pertussis* and has paralogs in *E. coli* (yhjD), M. tuberculosis and M. leprae (Fernandez & Weiss, 1994). The BrkB domain is highly conserved among both pathogenic and nonpathogenic mycobacteria, indicating that it may have a function that is crucial to survival, but has been altered to promote virulence in pathogenic bacteria. *Mycobacterium leprae*, which causes leprosy and cannot be grown in vitro due to the small size of its genome (1,604 protein-coding genes) contains an ortholog of Mtb-BrkB. Since the *M. leprae* genome is so parsed down to only genes which are necessary for its survival within a host, the presence of a BrkB ortholog suggests that BrkB plays an important role in host infection, *Mycobacterium smegmatis* (Msmeg) and *Mycobacterium marinum* (Mm), which are both commonly used model organisms to study Mtb, also both contain an ortholog of Mtb-BrkB. Msmeg is a non-pathogenic bacterium that shares >2,800 orthologs with >50% identity with Mtb (Sparks et al., 2023).

M. marinum shares >3,000 orthologs with >85% identity with Mtb, and infects zebrafish with a TB-like illness, making it a useful model for studying TB (Stinear et al., 2008). Previous research in the lab has shown that the Mm ortholog of Rv2707, MMAR_2006 or Mm-BrkB, is required for Mm intracellular and extracellular growth in zebrafish. A transposon mutant library of Mm mutants was constructed including a mutant with a transposon insertion in Mm-BrkB. Mm wildtype (WT), the transposon mutant Mm (MMAR_2006::Tn), and the transposon mutant with heterologously expressed Mtb-BrkB (Mtb complement) were used to infect zebrafish larvae. At five days post infection, zebrafish infected with MMAR_2006::Tn showed a lower bacterial burden compared to WT. The bacterial burden by Mtb complement infection showed no difference to WT (Fig. 4). This indicates that Mm-BrkB is required for Mm infection in zebrafish, and that Mtb-BrkB rescues infection in Mm-BrkB transposon insertion mutants, indicating Mtb-brkB plays a role in infection. As well, intramacrophage growth in zebrafish larvae was determined 2 days post infection. The average proportion of macrophages infected with ³5 bacterium after 2 days was significantly lower for MMAR_2006::Tn than WT. This indicates that the role of Mm-BrkB may be related to intramacrophage growth. Finally, MMAr_2006::Tn grew less than WT in the presence and absence of macrophages, indicating that Mm-BrkB's role in infection may have an extracellular component as well as an intramacrophage component. The behavior of the Mm ortholog of Mtb-BrkB in Mm infection of zebrafish can provide insights into the role of Mtb-BrkB in tuberculosis infection. Therefore, Mtb-BrkB is a possible virulence factor of interest, and may help Mtb survive in intracellular and extracellular environments in the host.

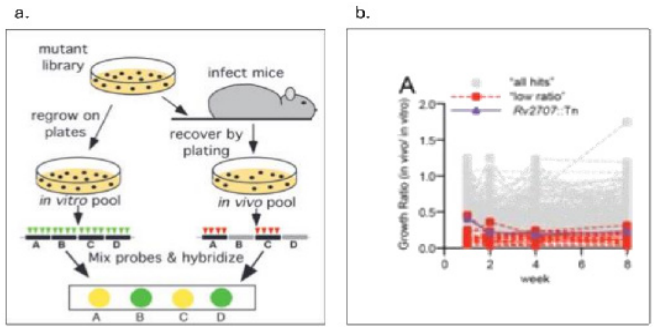

Figure 3. Mtb-BrkB transposon mutation attenuates infection in mice (Sassetti & Rubin, 2003).

(a) Sassetti and Rubin created a transposon mutant library and compared growth of transposon mutants *in vitro* and *in vivo*. (b) The growth ratio of *in vivo* to *in vitro* growth was plotted over time of infection in weeks and low ratio (<0.5) hits are highlighted in red. Mtb-BrkB transposon mutant indicated by blue line.

The structure of Mtb-BrkB is predicted to be a 6-transmembrane helix containing protein with cytosolic amino and carboxy termina by AlphaFold Server (Fig 5,6). Because Mtb-BrkB is a transmembrane protein of small size (~35kDa), this indicates that it may play a role in a larger protein complex that may be involved in transport across the inner membrane of Mtb.

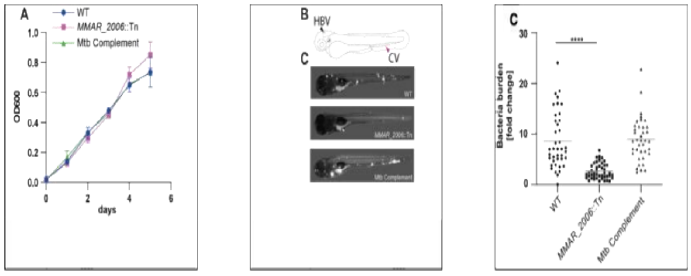

Figure 4. Mm-BrkB mutant shows attenuated growth in zebrafish, and Mtb-BrkB complement rescues infection.
(a) The optical density (OD600) of *in vitro* liquid culture of wild type *M. marinum* (WT), Mm-BrkB transposon insertion mutant (MMAR_2006::Tn), and Mm-BrkB mutant with Mtb-BrkB heterologously expressed (Mtb complement) was measured over time in days showing similar growth rate in vitro. (b) Zebrafish were infected via caudal vein (CV) and imaged five days post infection. (c) Bacterial burden in zebrafish infected with (MMAR_2006) Tn was significantly attenuated compared to WT, and Mtb complement rescued bacterial burden to WT level.

Introduction to Thesis Research

The goals of this study are to heterologously express and isolate Mtb-BrkB from E. coli for downstream functional and structural analysis. In order to do so, the expression of Mtb-BrkB in E. coli must be tested and optimized for growth, lysis, and elution conditions to achieve high yield of protein. This study used E. coli as a model organism, and it was transformed with a Mtb-BrkB coding plasmid vector. Another mycobacterial protein, Mtb-MscL, a mechanosensitive ion-channel, was used as a positive control throughout the study because it has previously been expressed and purified from E. coli (Chang et al., 1998). Mtb-MscL is, like Mtb-BrkB a small membrane protein, making it a good positive control.

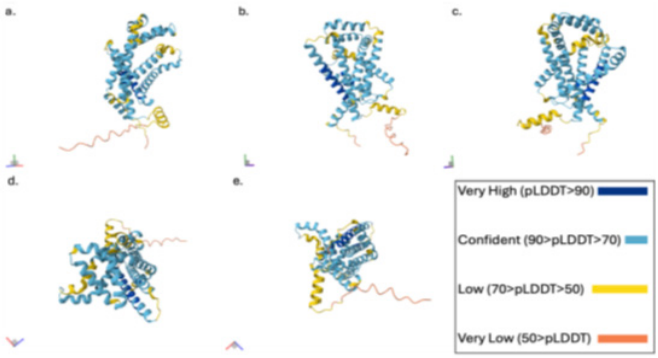

Figure 5. AlphaFold predicted structure of Mtb-BrkB from five perspectives.
The predicted structure of Mtb-BrkB is shown from front (a), turned 90° to the right (b), to the left (c), to the top (d), and to the bottom (e). the confidence of the prediction is given by the predicted local distance difference test (pLDDT) which measures the local confidence per residue.

Escherichia coli as a Model Organism

Escherichia coli (E. coli) is a bacillus gram-negative bacterium. *E. coli* is often used as a model organism in the laboratory because it has a relatively simple and well-studied genome as well as a fast replication time of ~20 minutes. Comparatively the replication time of Mtb is 16-24 hours. This makes *E. coli* a good model organism because it shortens growth time significantly. The general model of heterologous expression in *E. coli* starts with the transformation of *E. coli* with a plasmid containing a target protein coding sequence, an induction system, and an antibiotic resistance gene. The successfully transformed *E. coli* can then be selected for with inhibitory concentrations of antibiotic in growth media. In this case, ampicillin was used. The heterologous expression of the target protein can be turned on or induced by an inducing agent, and the *E. coli* can by lysed to extract and purify the target protein form the lysate (Fig. 7).

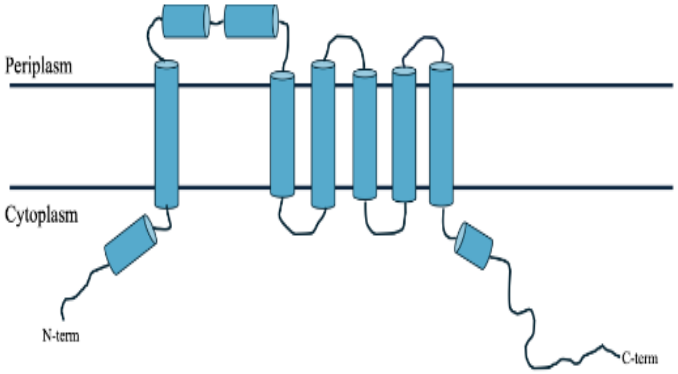

Figure 6. Simplified model of Mtb-BrkB.
Cylinders represent alpha-helices, and drawn lines are unstructured regions. The predicted protein structure has 6 transmembrane helices and 4 smaller helices, 2 cytoplasmic and 2 periplasmic. Both the N-terminal and the longer C-terminal tails are cytoplasmic.

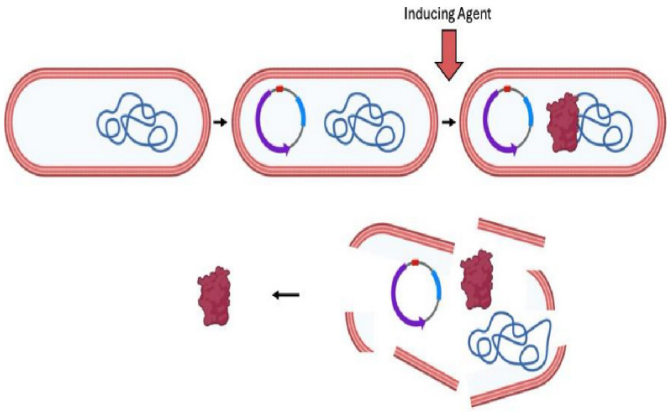

Figure 7. Overview of heterologous expression in E. coli.
Heterologous expression in E. coli is done by transforming E. coli with a protein-coding plasmid. E. coli will then express the target protein in the presence of an inducing agent (in this case, IPTG), and can by lysed. Target protein is then purified from crude lysate.

The strain of *E. coli* used to heterologous produce Mtb-BrkB was BL21(DE3) competent *E. coli*, which is a T7 expression strain of *E. coli*. Therefore, the BL21 *E. coli* produce the T7 RNA polymerase which will transcribe genes downstream of a T7 promoter, which is a common promoter on pET plasmid vectors. The T7 RNA polymerase gene is regulated by a *lacUV5* promoter which allows for expression of the T7 RNA polymerase in the presence of lactose or isopropyl β-D-1-thiogalactopyranoside (IPTG), allowing expression to be induced. It is also deficient in proteases Lon and OmpT, which prohibits the strain from degrading the heterologous produced proteins, leading to high protein yield (BL21(DE3) Competent *E. Coli* | NEB, n.d.).

However, there are some difficulties with using *E. coli* for the purpose of producing Mtb-BrkB. Membrane proteins are much harder to express in *E. coli* than cytosolic proteins, and membrane protein expression often leads to much lower yields. There are some strategies to overcome these difficulties including using *E. coli* strains optimized for protein expression such as BL21(DE3) E. coli, using solubilizing agents such as detergent or urea, and attaching solubility promoting tags to the target protein.

As well, *E. coli* inner membrane lipid composition is typically

made up of about 75% phosphatidylethanolamines (PE), about 20% phosphatidylglycerols (PG), and about 5% cardiolipins (CL) (Rowlett et al., 2017). Comparatively, the inner membrane lipid composition of Mtb is much more complicated. It contains glycerophospholipids phosphatidylinositol (PI), phosphatidylglycerol, phosphatidylserine (PS), phosphatidylethanolamine (PE), cardiolipin (CL), and mannosylated forms of PI known collectively as PIMs. As well, lipoaribomannans (LAMs) are anchored in the inner membrane (Jackson, 2014). Therefore, if the association of Mtb-BrkB is dependent on interaction with lipids which are found in the Mtb membrane and not the *E. coli* membrane, expression of Mtb-BrkB in *E. coli* might lead to aggregation of proteins. Despite the difference in membrane composition between *E. coli* and Mtb, expressing Mtb-BrkB in *E. coli* may be possible as suggested by the presence of a natively occurring BrkB ortholog in *E. coli* called YihY which is a membrane protein of unknown function which contains the BrkB domain.

Designing Plasmid DNA Constructs

A plasmid is a circular piece of DNA, that can be introduced to a bacterium via the process of transformation. Plasmids are useful because they introduce genes into the bacteria which will be transcribed and translated into proteins using the bacteria's cellular machinery. Two plasmids were constructed and used for the expression in *E. coli*: one plasmid containing Mtb-BrkB, and one plasmid containing Mtb-MscL (Fig. 8). Mtb-MscL is used as a positive control for the experiments since it is a Mtb protein which associated with the membrane. Mtb-MscL has previously been shown to be a gated ion-channel that forms a homohexamer (Chang et al., 1998). Since it was previously heterologously expressed in E. coli, it is used as a positive control for Mtb-BrkB.

The plasmid construct used to express Mtb-BrkB in *E. coli* uses the pET-21a(+) backbone. It includes an origin of replication (Ori), ampicillin resistance gene (*AmpR*), the lac I protein and lac O operator, the T7 promoter, the ribosome binding site (RBS) the Mtb-BrkB genetic sequence with a 6x-histidine tag. The origin of replication allows the plasmid to be replicated by the *E. coli*. The ampicillin resistance gene allows inhibitory concentrations of ampicillin to be used in order to select for the plasmid carrying *E. coli*. The lac I gene and lac O operator work in tandem to allow protein expression to be regulated based on the presence of lactose or IPTG. The lac I gene codes for the lac repressor protein which binds to the lac O operator, prohibiting transcription of the downstream genes. When lactose or IPTG are present, they will bind to the lac repressor protein causing a conformational change which will decrease its binding affinity to the lac O operator sequence, allowing the transcription of downstream sequences. The T7 promoter sequence signals for the T7 RNA polymerase produced by BL21 de3 *E. coli* to attach to the plasmid and begin transcribing. The T7 terminator sequence signals for the RNA polymerase to end transcription. The ribosome binding site signals for ribosomes to bind and begin translation of the mRNA to protein. Therefore, the protein which will be produced will be the Mtb-BrkB protein with 6 histidine residues at the carboxy terminus. The plasmid construct used to express Mtb-MscL is similar but uses the pET19b(+) backbone which has a different backbone sequence and different restriction sites. As well, the coding sequence will code for the Mtb-MscL protein with 10 histidine residues at the carboxy terminus.

Nickel Affinity Chromatography

The inclusion of the histidine tag on the carboxy terminus of the target proteins is useful for purification and isolation of the protein from cell lysates. This takes advantage of the affinity binding between the histidine amino acid and nickel ions. Positively charged nickel ions (Ni^{2+}) form non-covalent bonds with the nitrogen of the histidine residue (Fig. 9). Therefore, in a technique called nickel affinity chromatography, nickel ions associated on agarose beads can be used to selectively bind to the histidine residues of a His-tag. The proteins containing His-tags will bind to the beads, while other proteins in the clarified *E. coli* lysate will not. Then, imidazole, which has the structure of the histidine side chain (Fig. 9) can be used to disrupt and replace this bond to elute the purified protein fraction from the nickel beads. Therefore, using Nickel affinity chromatography, the heterologously expressed Mtb proteins can be purified for further functional or structural examination.

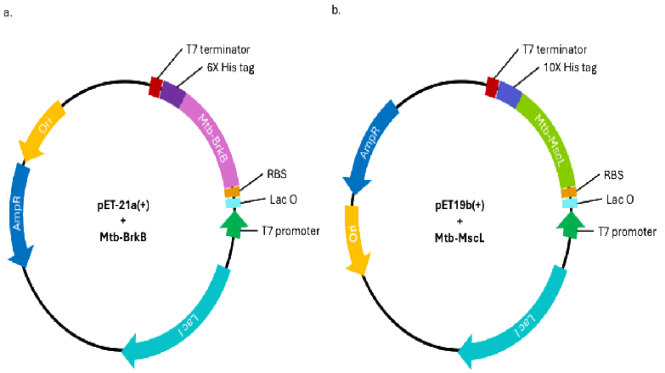

Figure 8. Design of Mtb-BrkB and Mtb-MscL plasmid vectors.
The design of the plasmid construct to express Mtb-BrkB (a) and Mtb-MscL (b) in BL21 E. coli both contain ampicillin resistance genes (AmpR), origins of replication (Ori), lac I repressor protein coding sequences (Lac I), lac O operators (lac O), ribosome binding sequences (RBS), multi-histidine tags (6X or 10X his tag), and T7 promoter and terminator sequences.

While it would be intuitive to perform a denaturing lysis based on the conclusion that denaturing lysis shows a slightly greater yield than native lysis (Fig. 11), we elected to use native lysis to maintain native structure of proteins. Based on personal communication with Dr. Keith Philibert, I expected the much larger scale growth conditions will compensate for the change in yield from denaturing to native lysis and produce plenty of protein to use in downstream analysis. E. coli was grown in 100ml cultures overnight before being transferred to 1L of broth. The optical density of the E. coli in the 1L cultures increased regularly over time, indicating no major effect of plasmid construct on growth (Fig. 13). After cultures reached optical densities of about 0.8 OD_{600}, they were spiked with 1mM IPTG. At the third hour (t=3), the culture was spiked with more IPTG to a total concentration of 1.5mM and then incubated for an additional 3 hours. Aliquots were taken from each condition at each hour (t=0,1,2,3,4,5,6). Protein expression of Mtb-BrkB and Mtb-MscL was determined by anti-6xHis Western blot. I expect that each aliquot aside from t=0 will contain either Mtb-BrkB (~35kDa) or Mtb-MscL (~15kDa) respectively with a possible upshoot in protein expression after the second IPTG spike at t=3hrs. The Western Blot showed the expression of Mtb-BrkB and Mtb-MscL at every time point, including a smaller band at t=0. The expression was even across the subsequent time points and did not show a clear increase at t=3 hrs in either condition. At every time point, Mtb-MscL was more abundantly expressed than Mtb-BrkB as indicated by thicker bands (Fig. 14). This indicates that induction of expression at 1L scale of Mtb-BrkB and Mtb-MscL was successful, however, adding additional IPTG does not increase protein expression.

Results

Recombinant E. coli yields low concentration Mtb-BrkB

We first sought to express Mtb-BrkB in E. coli and collect a purified fraction. We used a Mtb-BrkB expression system with induction by IPTG or lactose. As a control we performed the same experiments with MscL, a known mycobacterial membrane protein, and YxIM, an uncharacterized Bacillus subtilis cytoplasmic protein. We expected IPTG to induce a thicker band of protein in the lysate and to see a clear purified band in the elution. The presence of protein in the purified fraction is tested by SDS-PAGE. Because YxIM is not membrane associated, it may yield higher protein concentration, indicated by a thicker band at about 41 kDa. The presence of Mtb-BrkB and Mtb-MscL should be indicated by clear bands in the elution fractions at about 35kDa and 16kDa respectively. The elution fractions of both Mtb-BrkB and Mtb-MscL show a lot of unspecific binding bands and no clear band of expressed protein at the correct kDa weights. This indicates that there is very low expression of protein, and SDS-PAGE with

Coomassie staining may not be sensitive enough to detect presence of the recombinant proteins. On the other hand, the YxIM elution fraction shows a clear band in the at about 41kDa, indicating that YxIM was overexpressed in E. coli (Fig 10). Taken together, we concluded that Mtb-BrkB was not expressed highly or purified by this approach, however our approach was valid because we observed expression and purification of YxIM.

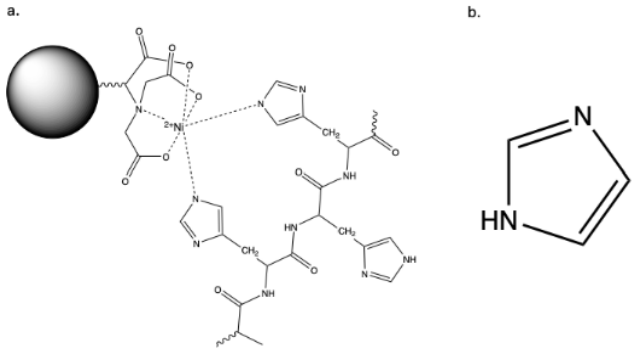

Figure 9. Poly-histidine tag affinity binding to Ni^{2+} beads compared to the structure of imidazole.
(a) The proton poor nitrogen of the histidine side chain will form non-covalent bonds with positively charged nickel ions which are coordinated to an agarose bead. (b) The structure of imidazole is the same as the side chain of a histidine residue, allowing for competitive elution.

Native lysis with detergent and denaturing lysis with urea showbands of different size and abundance

One possible explanation for the difference between Mtb-brkB expression and YxIM is that Mtb-BrkB is membrane-bound, making it more difficult to extract from the membrane. In order to break cell membranes more effectively and obtain higher protein yield, denaturing lysis with urea and sonication was compared to the previous lysis method which maintained the native protein shape with detergent and enzymatic cell lysis. Mtb-BrkB was purified from the lysates in either case by nickel affinity chromatography. The protein yield was compared visually by SDS-PAGE stained with Coomassie. The elution fraction of both shows bands at about 35kDa which indicates the presence of Mtb-BrkB. The elution fraction of the denatured lysate showed a slightly thicker band.

High concentrations of imidazole are necessary to elute Mtb-BrkB off Ni column

Given the presence of Mtb-BrkB and Mtb-MscL in cell lysates, I elected to move forward with target protein purification. In order to obtain a pure fraction of Mtb-BrkB and Mtb-MscL, cultures were lysed via emulsification and resuspended in detergent buffer for native conformation of protein. Previous results showed the optimal lysis of bacterial cells involved a denaturing solubilization with urea, but the optimal concentration of elution off nickel resin was still unknown. So, samples were run on a Ni^{2+} column, and the imidazole concentration was gradually increased from 25mM to 500mM as fractions were collected. UV-Vis spectrometry sample detection was used to measure the total protein absorbance at 280nm. The presence of protein should be indicated by an absorbance peak at 280nm, which will indicate in which fractions any protein was eluted. The chromatogram of absorbance at 280nm for the Mtb-BrkB elution shows a large peak at the end of the gradient at about 40 minutes, while the Mtb-MscL elution shows four scattered peaks between 20 and 35 minutes (Fig. 15). This indicates that a high concentration of imidazole is necessary to elute Mtb-BrkB off the nickel column.

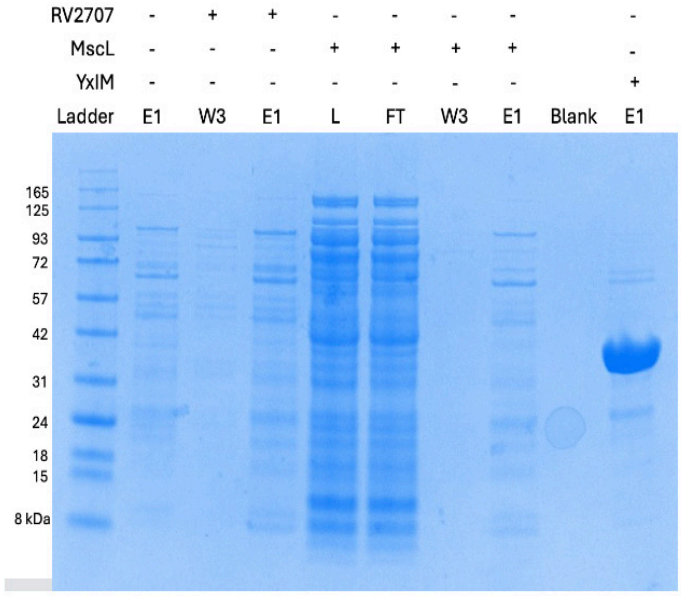

Fig. 10. Purification of Multi-His-tagged Rv2707, MscL, and YxIMs protein from recombinant E. coli show low yield of membrane proteins by SDS-PAGE.
(Lanes 2-4) The elution (E1) of Rv2707-6XHis off nickel resin columns show a very similar banding pattern to the untransformed E. coli which serves as a negative control, indicating low or no yield of Rv2707 from recombinant E. coli. (Lanes 5-8) The second experimental condition, MscL, also shows no clear induction of protein expression in the lysate (L) versus the flow through (FT), and no distinct bands in the elution (E1), indicating low to no yield of the MscL protein from recombinant E. coli. The banding pattern in lanes 2, 4, and 8 along with the clarity of both washes (lanes 3 and 7) also indicate that E. coli have native proteins which have high affinity to the charged nickel resin. The positive control, pWC101/YxIM, shows a dark band at the expected kDa weight of about ~41kDa in the elution (E1), indicating high protein expression in E. coli and high yield by nickel resin column purification.

The fractions of interest were then run on a gel and the presence of Mtb-BrkB and Mtb-MscL were tested by anti-6xHis Western Blot. The only fraction which showed the presence of Mtb-BrkB, as indicated by a band at about 35kDa, was fraction 2B6 which was near the end of the eluted fractions. All fractions tested (1E2, 1E3, 1F7, 1H6, 1H3, 1H1) showed the presence of Mtb-MscL as indicated by a band near 16kDa. The flow through (1A1) fraction in each did not show any protein in either condition (Fig 16). This indicates that the both Mtb-BrkB and Mtb-MscL bond to and then eluted off the nickel column, but Mtb-MscL was likely more abundant and eluted more easily off the column. In order to determine all the Mtb-BrkB containing fractions, a detailed examination of fractions near 2B6 was analyzed by a Western Blot as well. The last four fractions (2B7, 2B6, 2B5, and 2B4) showed the presence of Mtb-BrkB as indicated by the anti-6xHis specific band near the expected weight of 35kDa (Fig 17). This indicates that these fractions contain Mtb-BrkB, though there is low total quantity of Mtb-BrkB eluted off the nickel column. However, no protein was observed by Ponceau stain of the membrane, indicating low yield and no abundant contaminants in sample.

Mtb-BrkB induced at small- medium- and large-scale growth conditions

In order to test whether the induction of Mtb-BrkB expression was successful, a 5mL small-scale and then 50mL medium-scale growth conditions were performed and induced with 1mM IPTG. The cultures were then lysed with sonication in denaturing urea buffer, and the presence of Mtb-BrkB and Mtb-MscL was tested via anti-6xhis Western Blot. The small scale and medium scale conditions should show expression of Mtb-BrkB

at the expected kDa weight of about 35kDa and Mtb-MscL at about 16kDa. Both the small scale and medium scale growth conditions showed the presence of Mtb-BrkB and Mtb-MscL in the lysates while the medium scale growth condition showed a higher amount of total protein as indicated by the wider bands (Fig. 12). This indicates that induction of expression of Mtb-BrkB and Mtb-MscL was successful at both a 5ml and 50ml scale.

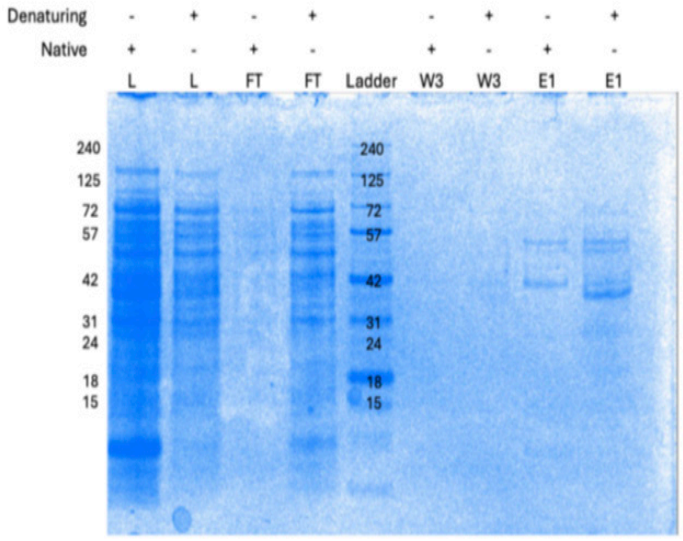

Figure 11. Denaturing lysis conditions yield greater protein abundance in elution fraction.
Native lysis of E. coli with 1% TritonX-100 was compared to denaturing lysis with 6M urea. Both lysates were purified via nickel affinity beads. Neither lysate (L) showed a clear band at about 35kDa indicating over-expression of Mtb-BrkB. The first elution fraction (E1) shows a and at about 35 kDa in both conditions. While the denaturing band is thicker, indicating greater protein yield, it is also at a slightly smaller kDa weight, indicating possible protein degradation.

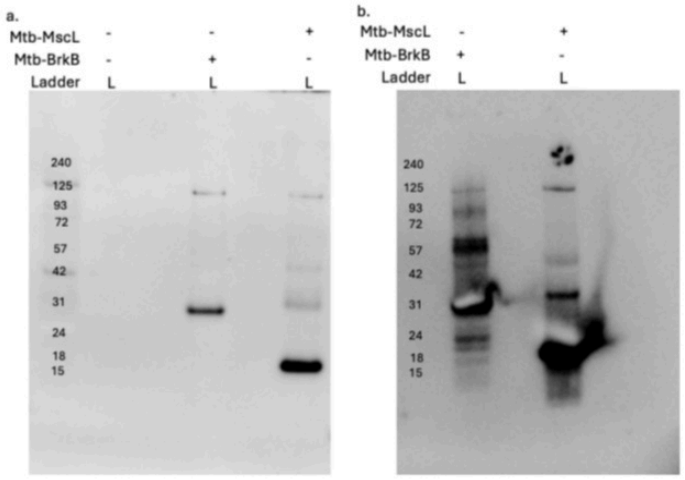

Figure 12. Small-scale (5ml) and medium scale (50ml) growth conditions both yield protein expression of Mtb-BrkB and Mtb-MscL.
E. coli was grown in 5ml small-scale cultures (a) and 50mL medium-scale cultures (b) and protein expression was induced via IPTG. E. coli cells were lysed via sonication and protein was denatured with urea and SDS. The presence of Mtb-BrkB in the lysate (L) is shown by a band near expected kDa weight (35kda), and Mtb-MscL by a band near expected kDa weight (16kDa).

Discussion

Mtb-BrkB Expresses in E. coli in the nanogram range

The heterologous expression of Mtb-BrkB was seen in E. coli in small-, medium-, and large-scale growth cultures and protein expression was induced by IPTG (Fig 8,9). Optimization of growth, lysis, and purification methods yielded some insights into protein expression methodology. Two different lysis strategies were employed: a manual cell breaking by sonication paired with a denaturing buffer to solubilize and denature the protein sample, and an enzymatic cell breaking with detergent to solubilize and maintain native structure of proteins. The denaturing lysis procedure showed slightly higher protein yield after purification (Fig. 7). However, an SDS-PAGE gel stained with Coomassie blue was used for determination of protein presence, which shows very faint banding and the difference between the abundance of protein in the native vs denatured conditions may have been due to random fluctuations in purification procedure. As well, the denatured condition showed a band at a slightly lower kDa weight than the enzymatic condition, indicating possible protein degradation. Overall, while denaturing with Urea and SDS is a useful tool for faster, possibly slightly more abundant protein yield, native lysis is better for downstream analysis because it limits protein degradation and the necessity for protein refolding. Finally, the concentration of imidazole needed to elute Mtb-BrkB off a nickel column was determined by FPLC elution with an imidazole gradient from 25mM to 500mM imidazole in sodium phosphate running buffer. The only fractions which were shown to contain Mtb-BrkB by Western Blot were the last four fractions of the gradient, indicating that high concentrations of imidazole are needed to elute Mtb-BrkB off the nickel column (Fig.10,12). Comparatively, Mtb-MscL eluted off the column much more easily, with the first elution peak at about 250mM imidazole (Fig. 10, 11). Previously, imidazole elution had been done with a single concentration of imidazole off nickel resin columns with 250mM imidazole. This may explain previous low yields of Mtb-BrkB off nickel resin in the pure fractions. However, because detection by Western Blot was not done, and a clear overexpression in the lysate was not seen, it is unknown how much protein was lost between the lysate and the pure eluted fractions.

Despite optimization efforts, the expression conditions yielded low abundance of Mtb-BrkB and Mtb-MscL in every case. This is clear based on the necessity of using Western Blot protein detection in order to see protein bands over Coomassie blue staining. The detection limit of InstantBlue Coomassie blue staining of protein gels is about 0.1ug of protein per band (Coomassie InstantBlue® (ISB1L) Protein Stain (Ab119211) | Abcam, n.d.). Comparatively, the detection limit using chemiluminescent detection of HRP-conjugate in Western Blot can be as low as 3pg of protein per band (Enzo Life Sciences, 2023). Therefore, the detection of Mtb-BrkB by Western Blot, but only faintly by Coomassie staining places the quantity of protein in the high nanogram range. Assuming the lowest detectable protein quantity by Coomassie staining, the concentration of Mtb-BrkB in the elution fractions is 20ug/ml, which is too low for most downstream analysis.

Limitations of Study

Because of time and budget constraints, there are optimization conditions which were not explicitly tested in the course of this study including the inducing agent, sonication vs emulsification, and detergent selection. First, we used IPTG as the inducing agent because it is commonly used with the T7 promotor system and because of ease of spiking cultures with relatively small volumes of IPTG. We could have tested the difference between inducing with lactose vs IPTG. Since lactose is the naturally occurring sugar off which the T7 system is based, it may have positive effects on E. coli culture growth. In another study, lactose was more effective at expressing recombinant proteins in E. coli and H. pylori than IPTG (Yan et al., 2004). This is likely because lactose is non-toxic to cells at even high concentrations, whereas IPTG can cause cell stress due to negative synergistic activity with anthropogenic toxins (Dvorak et al., 2015). However, the limitations of using lactose as an inducing agent include the variability in optimal lactose concentration for induction. As well, IPTG is more stable than lactose because it is not part of any natural metabolic pathways and will therefore not be used or broken down by cells. Secondly, the effect of manual cell breaking by sonication vs homogenization by microfluidizer was never studied. Sonication was used for cell breaking on small scale and medium scale cultures, but

due to consultation with Dr. Kieth Philibert at RFU, large scale cultures were lysed via microfluidizer. The microfluidizer was not used on the small- and medium- scale cultures because those were done prior to partnership with RFU, and we did not have access to a microfluidizer. Sonication was not used for the large volume lysis protocol because the efficiency of sonication may be reduced at high volumes due to factors such as increased distance of cells from probe and non-homogenous cell treatment. As well, homogenization by microfluidizer is more time efficient and effective at high volumes than sonication because it uses a continuous and constant flow to pass the cell suspension through the high-pressure chamber. The difference between sonication and emulsification was assumed to be negligible, but this assumption was never directly tested. Whether emulsification of cultures has an effect on protein yield or degradation compared to sonication is, therefore, unclear. Finally, the detergent selection for native lysis was not optimized due to time and cost restraints. The detergent used to solubilize protein was TritonX-100, which is a non-ionic surfactant. It is commonly used for protein extraction; however, other gentler detergent options may have been used. One such option is DDM or n-dodecyl b-D-maltoside which is commonly used to prepare native protein sample for native protein gels. DDM is gentler than TritonX-100 and may have been used to prevent protein degradation.

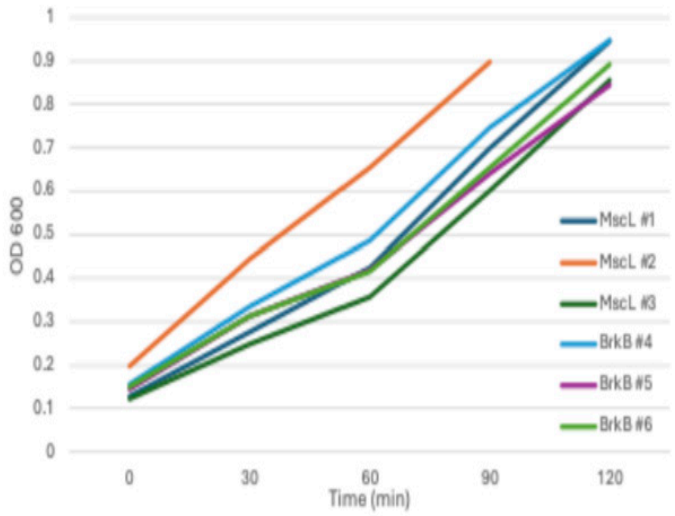

Figure 13. Growth curve of large-scale E. coli culture prior to IPTG induction.

1L cultures were inoculated with E. coli at t=0 min and incubated at 37°C for approximately 120 min before IPTG spiking. Three replicate flasks were grown for each condition (MscL, BrkB). The optical density (OD_{600}) of each flask was measured every 30 min. Flask 2 (orange) grew faster than the other flasks and was pulled from incubator at 90 min. The final optical density of every flask was between 0.84-0.95 OD_{600}.

The limitations of the study include the difficulty of expressing and purifying a small, membrane- embedded protein from E. coli. As discussed previously, the membrane structure of Mtb and E. coli vary, meaning the expression of Mtb-BrkB in the membrane of E. coli may be disrupted and lead to protein aggregation. Regardless, there are many different factors and decisions to be made when choosing and building an expression system for heterologous production of protein. The first of these factors is which organism to express the target protein in. I chose E. coli because of its fast replication time and well-established history of use as a model organism for protein expression. However, some other options could be used including yeast, Mycobacterium smegmatis, or Schneider 2 cells derived from Drosophila melanogaster. The advantages of using yeast for protein expression include cost effectiveness, and the ability to do high volume protein expression. Yeast, Saccharomyces cerevisiae, is often used to express eukaryotic proteins since it is a fast-growing eukaryotic cell, but it can be useful for prokaryotic protein expression as well. Compared to E. coli, S. cerevisiae was found to be more efficient at protein production of four integral membrane proteins, and in one case rescued protein production of a zinc transporter protein which was undetectable in E. coli (Preisler et al., 2021). Therefore, since Mtb-BrkB is not well expressed in E. coli, and is an integral membrane protein, it may be more highly expressed in yeast. M. smegmatis is another option for model organism. M. smegmatis is often used as the non-infectious, faster growing laboratory alternative to M. tuberculosis. Compared to E. coli, M. smegmatis's replication time is quite slow, 3 hrs. compared to E. coli's 20 min. However, the advantage of M. smegmatis is it is closely related to M. tuberculosis, and it has a BrkB ortholog which has high percent identity similarity to Mtb-BrkB. This means that Mtb-BrkB would likely be expressed and function similarly in M. smegmatis as it is in M. tuberculosis, which is helpful for both expression and functional analysis. The last potential option I explored was Schneider 2 or S2 cells derived from the fruit fly, Drosophila melanogaster. Schneider 2 cells are eukaryotic cells, so like yeast they are often used for eukaryotic protein expression. They also can use a temperature activated induction system Gal4/UAS which avoids the possible toxicity of a chemical induction system.

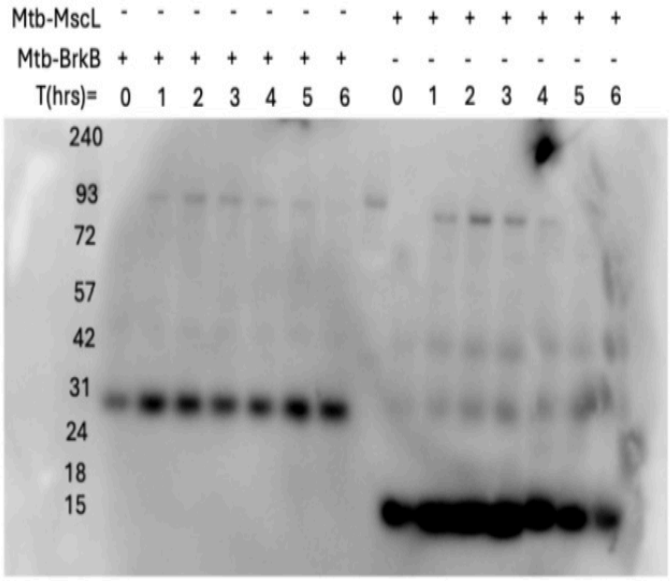

Figure 14. Large scale growth conditions show expression of Mtb-BrkB and Mtb-MscL at all time points.

E. coli was grown in 1L large-scale cultures protein expression was induced via IPTG at time(T)=0, 3 hrs. E. coli cells were lysed via emulsification. The presence of Mtb-BrkB in the lysate is shown by a band near expected kDa weight (35kda), and Mtb-MscL by a band near expected kDa weight (16kDa).

Secondly, while Mtb-BrkB is the protein of interest, we could have used an ortholog from a different Mycobacterium for expression and downstream analysis. The two salient options I explored were M. smegmatis and M. thermoresistibile. The M. smegmatis BrkB ortholog (Ms-BrkB) has 70% identity, and the M. thermoresistibile BrkB ortholog (Mth-BrkB) has 71% identity with Mtb-BrkB (NCBI BLAST). Therefore, both orthologs are closely related to the Mtb-BrkB protein and likely have similar structures and functions. The main advantage of using Ms-BrkB would be if M. smegmatis was also used as the model organism because it is the natively occurring BrkB ortholog, making expression less stressful for the bacterium. M. thermoresistibile (Mth) is a thermophilic mycobacterium. Mth proteins are more thermoresistant, often more soluble, and structurally similar to their Mtb orthologs, making is a useful source of orthologs for crystallography (Edwards et al., 2012)Mycobacterium tuberculosis (Mtb. Therefore, while it makes sense to use Mtb-BrkB because it is the actual protein of interest native to Mtb, expressing Mth-BrkB could be useful for downstream structural analysis, and because it is so similar to Mtb-BrkB, Mth-BrkB would give a good representation of the structure of Mtb-BrkB.

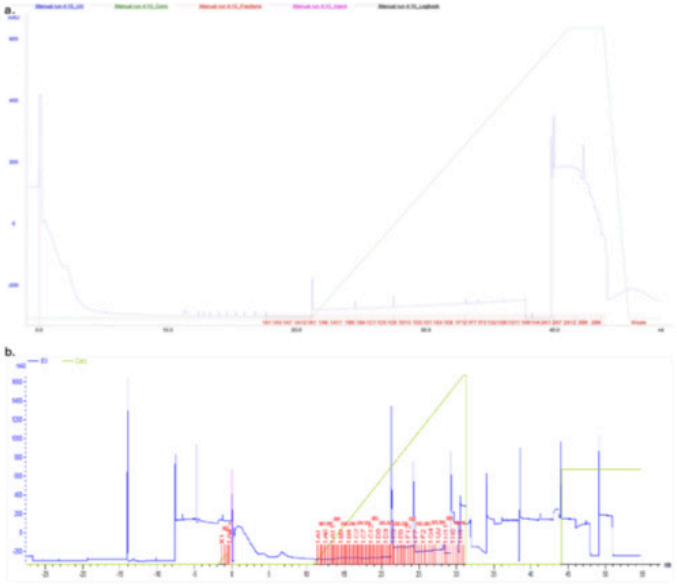

Figure 15. Chromatogram of Absorbance at 280nm over 25mM to 500mM imidazole gradient elution of Mtb-BrkB (a) and Mtb-MscL(b) through nickel column.
The absorbance at 280nm (blue; y-axis) was measured over time (x-axis) to determine the presence of protein in elution off a nickel column over time. The concentration of imidazole (green) gradually changed from 25mM to 500mM in the running buffer over about 40minutes. The protein and running buffer were run through the column at 1ml/min. Mtb-brkB elution (a) showed one large peak near the end of the elution at about 40 min. The Mtb-MscL elution (b) shows 4 sharp peaks at about 21, 25, 29,32 min. Collected factions are indicated in red.

Additionally, there are multiple possible induction system used for E. coli including the T7 system which was the one used in this study. The LacO system includes the LacI repressor and the Lac operator which allow protein expression to be turned on with the addition of lactose or IPTG. The advantage of this system is it is simple, cost effective, and combined with the T7 promoter system has high levels of expression. However, the lac operon is also “leaky” or in other words, repression of gene expression is not tightly controlled by the absence of lactose or IPTG, and some protein expression may occur prior to spiking. This is seen in the large-scale culture because some protein expression of Mtb-BrkB and Mtb-MscL is seen at t=0 (Fig. 9). Another possible option is the pBAD promoter system which includes the araBAD operon and the araC regulatory protein. The araC protein acts as both a repressor and activator in this system. When arabinose, a pentose sugar, is absent, araC inhibits RNA binding and gene expression, and when arabinose is present araC undergoes a conformational change which allows it to enhance RNA binding. The advantage of this system is because araC is both a repressor and an activator it is much less “leaky” than the lacO system, and expression is positively associated with the concentration of arabinose added allowing for graded expression (Guzman et al., 1995). Finally, a new Self-Inducible Expression (SILEX) system may be a cost effective and simple alternative to the lacO system. The silex system contains a plasmid coding for the human heat shock protein 70 (hHsp70) and another pET-T7 plasmid with the target protein. The hHsp70 protein interacts with endogenous GAPDH in the E. coli to autoinducer the target protein without the addition of lactose or IPTG (Briand et al., 2016) medical and industrial cell factory for recombinant protein production. The inducible lac promoter is one of the most commonly used promoters for heterologous protein expression in E. coli. Isopropyl-β-D-thiogalactoside (IPTG. The advantage of this system is the simplicity of autoinduction. Because spiking is not required, the monitoring of optical density of the E. coli culture and spiking at the right growth phase is unnecessary. However, it is relatively less studied and used than the lacO system.

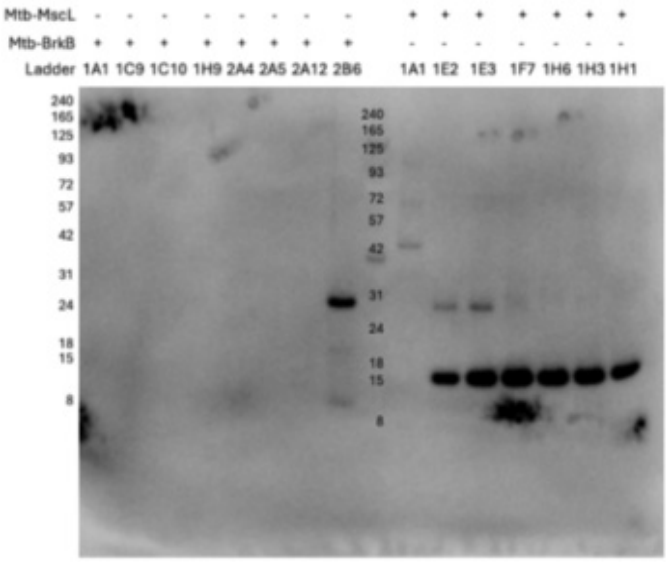

Figure 16. Elution factions show presence of Mtb-BrkB and Mtb-MscL via anti-his tag Western Blot.
E. coli was grown in 1L large-scale cultures protein expression was induced via IPTG. E. coli cells were lysed via emulsification and then run on a nickel column with imidazole gradient elution. The presence of Mtb-BrkB in the one elution fraction 2B6 is shown by a band near expected kDa weight (35kda), and Mtb-MscL by a band near expected kDa weight (16kDa).

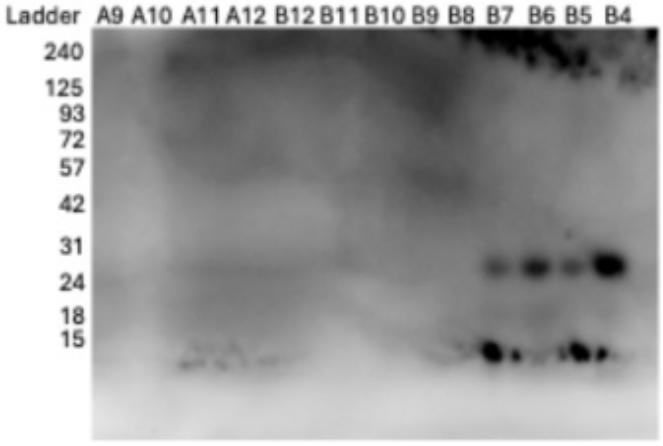

Figure 17. Detailed examination of Mtb-BrkB fractions reveals four fractions with protein.
E. coli was grown in 1L large-scale cultures protein expression was induced via IPTG. E. coli cells were lysed via emulsification and then run on a nickel column with imidazole gradient elution. The presence of Mtb-BrkB in all fractions near 2B6 was examined. Four fractions (2B7, 2B6, 2B5, and 2B4) showed faint bands at about 35kDa indicating the presence of Mtb-BrkB.

Finally, the tag used may affect both the solubility and the purification of the target protein. We chose the 6X-His tag which added 6 histidine residues to the C-terminal end of the target protein. This tag is advantageous because of its small size, its high binding affinity to metal ions such as Ni^{2+} and the low abundance of naturally occurring histidine residue repeats (Puckett, 2015). Its small size (0.8kDa) means that it likely does not cause conformational change to the target protein, and the Nickel affinity allows for a relatively simple purification method, making the 6X-His tag a common tag for protein purification. However, the 6X-His tag has no effect on protein solubility. On the other hand, a maltose-binding protein (MBP) tag can be used to enhance solubility and has native affinity to

maltose, so maltose containing resin can be used to purify the target protein (Kapust & Waugh, 1999). However, the MBP tag is quite bulky (43kDa), which means it must be cleaved off for further structural or functional analysis. Using MBP as a tag could be useful for Mtb-BrkB since it is a non-soluble protein. By using the MBP tag, we could functionally make Mtb-BrkB soluble, which would make it less stressful for E. coli to produce and much easier to isolate and purify from the crude lysate. The above information is summarized in Figure 18, which highlights some advantages of each method and outlines the methods chosen for this study in red.

Future Directions

The future directions of this study include revisiting optimization of expression conditions in order to produce Mtb-BrkB in high abundance. As discussed above, I may change the model organism, induction system or affinity tag of my expression system in order to increase expression. Currently, the most promising change may be introducing a cleavable MBP tag which would help solubilize Mtb-BrkB, since much of the difficulty of expressing Mtb-BrkB arose because it is a membrane protein. If even a solubility tag does not increase yield, then a wholesale change of the model organism and expression system may be necessary to express Mtb-BrkB in high abundance. However, once that is accomplished, the ultimate goal is structural and functional analysis.

Structural analysis of Mtb-BrkB will examine the stoichiometry and structure of Mtb-BrkB. To analyze the sub-cellular stoichiometry of Mtb-BrkB, a multimerization experiment using crosslinking reagent disuccinimidyl substrate (DSS) can be performed, as was done to show that Mtb-MscL forms a homohexamer within the cell (Chang et al., 1998). Because Mtb-BrkB is a relatively small membrane protein like Mtb-MscL, it may also form a homomultimer to form a pore or cross-membrane signaling complex. As well, structural analysis can be done via X-ray crystallography or cryo-electron microscopy. To do so, the Mth-BrkB may be used since it is likely more thermostable. The multimeric structure of Mtb-BrkB may give insights to the function of Mtb-BrkB as a virulence factor. However, Mtb-BrkB may also form a complex with other proteins which the multimerization experiment would not reveal.

Materials and Methods

Bacterial Culture and Growth

Briefly, competent BL21(DE3) E. coli were transformed with pET-21a(+) + Mtb-BrkB or pET19b(+) + Mtb-MscL and grown on LB agar +100ug/ml ampicillin plates overnight at 37°C. Single colonies were picked, to inoculate LB broth culture +100ug/ml ampicillin and incubated at 37°C and 220rpm on a shaking platform until it reached an optical density of about 0.8 OD_{600}. The starter culture is then used to inoculate 5mL, 50mL, or 1L LB broth +100ug/ml ampicillin culture and incubated at 25°C (for small- and medium-scale) or 16°C (for large-scale) at 150rpm until optical density of about 1.0 OD_{600} reached. The cultures were then spiked with 1mM isopropyl b-D-thiogalactopyranoside (IPTG) and incubated for an additional 6-16hrs.

Cell Lysis and Protein Extraction

Briefly, The E. coli cultures were centrifuges at 7,000xg for 30 minutes and the pellet was stored in -20°C until use. The cell breaking was approached in two ways over the course of this study: native lysis, and denaturing lysis. Native lysis with enzymatic cell breaking proceeded as follows: the pellet was resuspended in native lysis buffer (50mM sodium phosphate buffer pH 8, 200mM NaCl, 1% TritonX-100), and working concentrations of lysozyme, DNase, and EDTA-free protease inhibitor were added, and cell suspension was incubated at 37°C for 45mins mixing gently on shaking platform. Lysate was clarified by centrifugation at 7,000xg for 30 min. Denaturing lysis with sonication proceeded as follows: the pellet was resuspended in denaturing buffer (50mM sodium phosphate buffer pH 8, 200mM NaCl, 6M Urea). Cell suspension was sonicated on ice in 5x30 sec bursts 5 sec on/5 sec off with 2-min breaks in between. Lysate was clarified by centrifugation at 7,000xg for 30 min. Native lysis with homogenization by microfluidizer was performed as follows: the pellet was resuspended in lysis buffer (50mM sodium phosphate buffer pH 8, 200mM NaCl) and passed through Avestin Emusiflex C3 Microfluidizer at 5,000psi to remove cell clumps. Cell suspension was then passed through microfluidizer twice more at 15,000psi to break cells. Immediately, 1% (w/v) TritonX-100 was added, and sample was incubated at room temp for 15 minutes with gentle shaking. The lysate was clarified by centrifugation at 15,000xg for 15 min. The details of which lysis method was used for each experiment are given in figure legends.

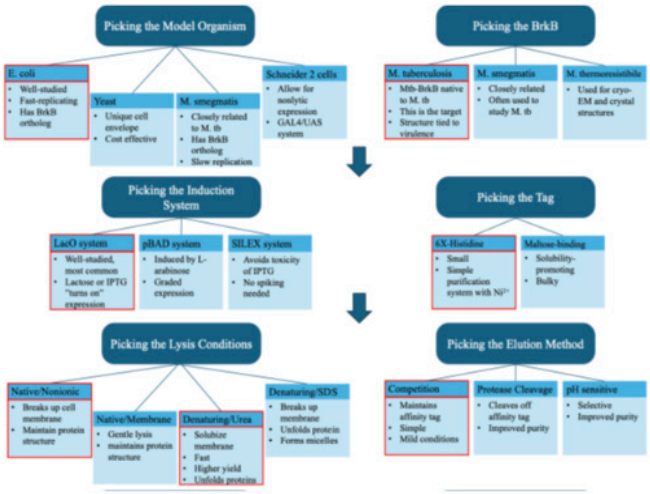

Figure 18. Tree of decisions for building a complete heterologous expression system.

The first level of building a heterologous expression system is picking the target protein and the model organism in which to express it. The model organism informs the induction system used, and the target protein sequence is edited to include a N-terminal or C-terminal tag. The model organism and induction system inform the growth, induction, and lysis conditions of the study and the tag informs the purification method. The methods used in this study are outlined in red at each step.

Purification of Mtb-BrkB by Nickel Affinity Chromatography

Briefly, about 12X-CV clarified lysate was added to Ni-NTA resin and incubated overnight at 4°C with constant nutation. Lysate and resin slurry was added to 1mL spin column and centrifuged at 800xg for 1 min. The resin was washed with 5X-CV wash buffer (50mM sodium phosphate buffer pH 8, 200mM NaCl, 10mM imidazole), incubated at room temp. for 5 min. with gentle nutation, and centrifuged at 800xg for 1 min. Wash was repeated a total of three times. Protein was eluted off Ni-NTA resin with 2X-CV with elution buffer (50mM sodium phosphate buffer pH 8, 200mM NaCl, 250mM imidazole) and centrifuged an 800xg for 1 min. Elution was repeated a total of three times. Eluted fractions were stored short-term at -20°C until use.

Imidazole Gradient Elution with FPLC

Briefly, a 1mL His-trap FF column was attached to FPLC and washed with 5X-CV water at 1ml/min. Column is equilibrated with 5X-CV binding buffer (20mM Sodium Phosphate, 500mM NaCl, 25mM Imidazole, pH 7.4) at 1 ml/min before injection of 2mL Mtb-BrkB or Mtb-MscL clarified lysate using a luer lock syringe. The column is then washed with 10-15X-CV at 1ml/min. The sample elution gradient from 0-100% elution buffer (20mM Sodium Phosphate, 500mM NaCl, 500mM Imidazole, pH 7.4), and 100uL fractions were collected in a deep 96-well plate following a snake-like pattern.

SDS-PAGE and Western Blot

Briefly, samples were combined with 1X LDS loading buffer and b-mercaptoethanol before being loaded onto 4-12% Bis-Tris protein

gel with 1X MES running buffer. BluEye pre-stained protein ladder was used. Samples were run on gel at 120V for 1hr. Protein gels were then either stained with InstantBlue Coomassie blue stain for 15min-1hr and imaged or transferred onto nitrocellulose membrane for Western Blot. Western Blots were performed with semidry apparatus and blotted with 1° monoclonal mouse anti-6X-His antibodies, and 2° monoclonal goat anti-mouse horseradish peroxidase (HRP) conjugated antibodies. Western Blots were visualized using ECL substrate and chemiluminescence.

References

1. Barberis, I., Bragazzi, N. L., Galluzzo, L., & Martini, M. (2017). The history of tuberculosis: From the first historical records to the isolation of Koch's bacillus. Journal of Preventive Medicine and Hygiene, 58(1), E9–E12.
2. Bartlett, A., Padfield, D., Lear, L., Bendall, R., & Vos, M. (2022). A comprehensive list of bacterial pathogens infecting humans. Microbiology, 168(12). https://doi.org/10.1099/mic.0.001269
3. Bendre, A. D., Peters, P. J., & Kumar, J. (2021). Tuberculosis: Past, present and future of the treatment and drug discovery research. Current Research in Pharmacology and Drug Discovery, 2, 100037. https://doi.org/10.1016/j.crphar.2021.100037
4. Betts, J. C., Lukey, P. T., Robb, L. C., McAdam, R. A., & Duncan, K. (2002). Evaluation of a nutrient starvation model of Mycobacterium tuberculosis persistence by gene and protein expression profiling. Molecular Microbiology, 43(3), 717–731. https://doi.org/10.1046/j.1365-2958.2002.02779.x
5. BL21(DE3) Competent E. coli | NEB. (n.d.). Retrieved April 26, 2025, from https://www.neb.com/en-us/products/c2527-bl21de3-competent-e-coli?srsltid=AfmBOopWp-CoRe5j45Vh208XRPDvRfVxJHec1L03BUAJqABSZ96seXqo
6. Briand, L., Marcion, G., Kriznik, A., Heydel, J. M., Artur, Y., Garrido, C., Seigneuric, R., & Neiers, F. (2016). A self-inducible heterologous protein expression system in Escherichia coli. Scientific Reports, 6(1), 33037. https://doi.org/10.1038/srep33037
7. Cambier, C. J., Falkow, S., & Ramakrishnan, L. (2014). Host Evasion and Exploitation Schemes of Mycobacterium tuberculosis. Cell, 159(7), 1497–1509. https://doi.org/10.1016/j.cell.2014.11.024
8. Cambier, C. J., Takaki, K. K., Larson, R. P., Hernandez, R. E., Tobin, D. M., Urdahl, K. B., Cosma, C. L., & Ramakrishnan, L. (2014). Mycobacteria manipulate macrophage recruitment through coordinated use of membrane lipids. Nature, 505(7482), 218–222. https://doi.org/10.1038/nature12799
9. CDC. (2024, November 7). National Data. Reported Tuberculosis in the United States, 2023. https://www.cdc.gov/tb-surveillance-report-2023/summary/national.html
10. Chandra, A., Kumar, R., Kant, S., Parthasarathy, R., & Krishnan, A. (2020). Direct and indirect patient costs of tuberculosis care in India. Tropical Medicine & International Health, 25(7), 803–812. https://doi.org/10.1111/tmi.13402
11. Chang, G., Spencer, R. H., Lee, A. T., Barclay, M. T., & Rees, D. C. (1998). Structure of the MscL Homolog from Mycobacterium tuberculosis: A Gated Mechanosensitive Ion Channel. Science, 282(5397), 2220–2226. https://doi.org/10.1126/science.282.5397.2220
12. Coomassie InstantBlue® (ISB1L) Protein Stain (ab119211) | Abcam. (n.d.). Retrieved April 8, 2025, from https://www.abcam.com/en-us/products/reagents/instantblue-coomassie-protein-stain-isb1l-ab119211#overlay=images
13. Dulberger, C. L., Rubin, E. J., & Boutte, C. C. (2020). The mycobacterial cell envelope—A moving target. Nature Reviews Microbiology, 18(1), 47–59. https://doi.org/10.1038/s41579-019-0273-7
14. Dvorak, P., Chrast, L., Nikel, P. I., Fedr, R., Soucek, K., Sedlackova, M., Chaloupkova, R., de Lorenzo, V., Prokop, Z., & Damborsky, J. (2015). Exacerbation of substrate toxicity by IPTG in Escherichia coli BL21(DE3) carrying a synthetic metabolic pathway. Microbial Cell Factories, 14(1), 201. https://doi.org/10.1186/s12934-015-0393-3
15. Edwards, T. E., Liao, R., Phan, I., Myler, P. J., & Grundner, C. (2012). Mycobacterium thermoresistibile as a source of thermostable orthologs of Mycobacterium tuberculosis proteins. Protein Science: A Publication of the Protein Society, 21(7), 1093–1096. https://doi.org/10.1002/pro.2084
16. Etiology of Tuberculosis | Clinical Infectious Diseases | Oxford Academic. (n.d.). Retrieved January 21, 2025, from https://academic.oup.com/cid/article/4/6/1270/288239
17. Fernandez, R. C., & Weiss, A. A. (1994). Cloning and sequencing of a Bordetella pertussis serum resistance locus. Infection and Immunity, 62(11), 4727–4738. https://doi.org/10.1128/iai.62.11.4727-4738.1994
18. Gandhi, N. R., Nunn, P., Dheda, K., Schaaf, H. S., Zignol, M., Soolingen, D. van, Jensen, P., & Bayona, J. (2010). Multidrug-resistant and extensively drug-resistant tuberculosis: A threat to global control of tuberculosis. The Lancet, 375(9728), 1830–1843.https://doi.org/10.1016/S0140-6736(10)60410-2
19. Global mortality associated with 33 bacterial pathogens in 2019: A systematic analysis for the Global Burden of Disease Study 2019. (2022). Lancet (London, England), 400(10369), 2221–2248. https://doi.org/10.1016/S0140-6736(22)02185-7
20. Guzman, L. M., Belin, D., Carson, M. J., & Beckwith, J. (1995). Tight regulation, modulation, and high-level expression by vectors containing the arabinose PBAD promoter. Journal of Bacteriology, 177(14), 4121–4130.
21. Hoft, D. F., Blazevic, A., Selimovic, A., Turan, A., Tennant, J., Abate, G., Fulkerson, J., Zak, D. E., Walker, R., McClain, B., Sadoff, J., Scott, J., Shepherd, B., Ishmukhamedov, J., Hokey, D. A., Dheenadhayalan, V., Shankar, S., Amon, L., Navarro, G., … Steinberg, S. (2016). Safety and Immunogenicity of the Recombinant BCG Vaccine AERAS-422 in Healthy BCG-naïve Adults: A Randomized, Active-controlled, First-in-human Phase 1 Trial. eBioMedicine, 7, 278–286. https://doi.org/10.1016/j.ebiom.2016.04.010
22. How do you Choose the Right Western Blot Detection Method? (n.d.). Enzo. Retrieved April 8, 2025, from https://www.enzo.com/note/how-do-you-choose-the-right-western-blot-detection-method/
23. Huszár, S., Chibale, K., & Singh, V. (2020). The quest for the holy grail: New antitubercular chemical entities, targets and strategies. Drug Discovery Today, 25(4), 772–780. https://doi.org/10.1016/j.drudis.2020.02.003
24. Inadequate housing and pulmonary tuberculosis: A systematic review | BMC Public Health | Full Text. (n.d.). Retrieved April 13, 2025, from https://bmcpublichealth.biomedcentral.com/articles/10.1186/s12889-022-12879-6#Sec7
25. Jackson, M. (2014). The Mycobacterial Cell Envelope—Lipids. Cold Spring Harbor Perspectives in Medicine, 4(10), a021105.https://doi.org/10.1101/cshperspect.a021105
26. Kapust, R. B., & Waugh, D. S. (1999). Escherichia coli maltose-binding protein is uncommonly effective at promoting the solubility of polypeptides to which it is fused. Protein Science, 8(8), 1668–1674. https://doi.org/10.1110/ps.8.8.1668
27. Koch, R., Brock, T. D., & Fred, E. B. (1982). The Etiology of Tuberculosis. Reviews of Infectious Diseases, 4(6), 1270–1274.
28. Lee, R. E., Brennan, P. J., & Besra, G. S. (1996). Mycobacterium tuberculosis Cell Envelope. In T. M. Shinnick (Ed.), Tuberculosis (pp. 1–27). Springer. https://doi.org/10.1007/978-3-642-80166-2_1
29. Locey, K. J., & Lennon, J. T. (2016). Scaling laws predict global microbial diversity. Proceedings of the National Academy of Sciences, 113(21), 5970–5975. https://doi.org/10.1073/pnas.1521291113
30. LUCA, S., & MIHAESCU, T. (2013). History of BCG Vaccine. Mædica, 8(1), 53–58.

31. Ndiaye, B. P., Thienemann, F., Ota, M., Landry, B. S., Camara, M., Dièye, S., Dieye, T. N., Esmail, H., Goliath, R., Huygen, K., January, V., Ndiaye, I., Oni, T., Raine, M., Romano, M., Satti, I., Sutton, S., Thiam, A., Wilkinson, K. A., … MVA85A 030 trial investigators. (2015). Safety, immunogenicity, and efficacy of the candidate tuberculosis vaccine MVA85A in healthy adults infected with HIV-1: A randomised, placebo-controlled, phase 2 trial. The Lancet. Respiratory Medicine, 3(3), 190–200. https://doi.org/10.1016/S2213-2600(15)00037-5

32. Preisler, S. S., Wiuf, A. D., Friis, M., Kjaergaard, L., Hurd, M., Becares, E. R., Nurup, C. N., Bjoerkskov, F. B., Szathmáry, Z., Gourdon, P. E., Calloe, K., Klaerke, D. A., Gotfryd, K., & Pedersen, P. A. (2021). Saccharomyces cerevisiae as a superior host for overproduction of prokaryotic integral membrane proteins. Current Research in Structural Biology, 3, 51–71. https://doi.org/10.1016/j.crstbi.2021.02.001

33. Prevalence of extrapulmonary tuberculosis and factors influencing successful treatment outcomes among notified cases in South India | Scientific Reports. (n.d.). Retrieved April 13, 2025, from https://www.nature.com/articles/s41598-025-92613-5

34. Puckett, M. C. (2015). Hexahistidine (6xHis) fusion-based assays for protein-protein interactions. Methods in Molecular Biology (Clifton, N.J.), 1278, 365–370. https://doi.org/10.1007/978-1-4939-2425-7_23

35. Ratcliffe, H. L., & Wells, W. F. (1948). TUBERCULOSIS OF RABBITS INDUCED BY DROPLET NUCLEI INFECTION. The Journal of Experimental Medicine, 87(6), 575–584.

36. Reis-Santos, B., Locatelli, R., Oliosi, J., Sales, C. M., do Prado, T. N., Shete, P. B., Riley, L. W., & Maciel, E. L. (2022). A Matter of Inclusion: A Cluster-Randomized Trial to Access the Effect of Food Vouchers Versus Traditional Treatment on Tuberculosis Outcomes in Brazil. The American Journal of Tropical Medicine and Hygiene, 107(6), 1281–1287. https://doi.org/10.4269/ajtmh.21-1074

37. Results of directly observed short-course chemotherapy in 112,842 Chinese patients with smear-positive tuberculosis. China Tuberculosis Control Collaboration. (1996). Lancet (London, England), 347(8998), 358–362.

38. Rowlett, V. W., Mallampalli, V. K. P. S., Karlstaedt, A., Dowhan, W., Taegtmeyer, H., Margolin, W., & Vitrac, H. (2017). Impact of Membrane Phospholipid Alterations in Escherichia coli on Cellular Function and Bacterial Stress Adaptation. Journal of Bacteriology, 199(13), e00849-16. https://doi.org/10.1128/JB.00849-16

39. Salari, N., Kanjoori, A. H., Hosseinian-Far, A., Hasheminezhad, R., Mansouri, K., & Mohammadi, M. (2023). Global prevalence of drug-resistant tuberculosis: A systematic review and meta-analysis. Infectious Diseases of Poverty, 12(1), 57. https://doi.org/10.1186/s40249-023-01107-x

40. Saqib, M., Khatri, R., Singh, B., Gupta, A., Kumar, A., & Bhaskar, S. (2016). Mycobacterium indicus pranii as a booster vaccine enhances BCG induced immunity and confers higher protection in animal models of tuberculosis. Tuberculosis, 101, 164–173. https://doi.org/10.1016/j.tube.2016.10.002

41. Sassetti, C. M., & Rubin, E. J. (2003). Genetic requirements for mycobacterial survival during infection. Proceedings of the National Academy of Sciences, 100(22), 12989–12994.https://doi.org/10.1073/pnas.2134250100

42. Sparks, I. L., Derbyshire, K. M., Jacobs, W. R., & Morita, Y. S. (n.d.). Mycobacterium smegmatis: The Vanguard of Mycobacterial Research. Journal of Bacteriology, 205(1), e00337-22. https://doi.org/10.1128/jb.00337-22

43. Stinear, T. P., Seemann, T., Harrison, P. F., Jenkin, G. A., Davies, J. K., Johnson, P. D. R., Abdellah, Z., Arrowsmith, C., Chillingworth, T., Churcher, C., Clarke, K., Cronin, A., Davis, P., Goodhead, I., Holroyd, N., Jagels, K., Lord, A., Moule, S., Mungall, K., … Cole, S. T. (2008). Insights from the complete genome sequence of Mycobacterium marinum on the evolution of Mycobacterium tuberculosis. Genome Research, 18(5), 729–741.

44. Teo, A. K. J., Singh, S. R., Prem, K., Hsu, L. Y., & Yi, S. (2021). Duration and determinants of delayed tuberculosis diagnosis and treatment in high-burden countries: A mixed-methods systematic review and meta-analysis. Respiratory Research, 22, 251. https://doi.org/10.1186/s12931-021-01841-6

45. Walley, J. D., Khan, M. A., Newell, J. N., & Khan, M. H. (2001). Effectiveness of the direct observation component of DOTS for tuberculosis: A randomised controlled trial in Pakistan. The Lancet, 357(9257), 664–669. https://doi.org/10.1016/S0140-6736(00)04129-5

46. Wingfield, T., Tovar, M. A., Huff, D., Boccia, D., Montoya, R., Ramos, E., Datta, S., Saunders, M. J., Lewis, J. J., Gilman, R. H., & Evans, C. A. (2017). A randomized controlled study of socioeconomic support to enhance tuberculosis prevention and treatment, Peru. Bulletin of the World Health Organization, 95(4), 270–280. https://doi.org/10.2471/BLT.16.170167

47. Wingfield, T., Tovar, M. A., Huff, D., Boccia, D., Montoya, R., Ramos, E., Lewis, J. J., Gilman, R. H., & Evans, C. A. (2016). The economic effects of supporting tuberculosis-affected households in Peru. The European Respiratory Journal, 48(5), 1396–1410.https://doi.org/10.1183/13993003.00066-2016

48. Yan, J., Zhao, S.-F., Mao, Y.-F., & Luo, Y.-H. (2004). Effects of lactose as an inducer on expression of Helicobacter pylori rUreB and rHpaA, and Escherichia coli rLTKA63 and rLTB. World Journal of Gastroenterology : WJG, 10(12), 1755–1758. https://doi.org/10.3748/wjg.v10.i12.1755